

ANALYSIS OF RÖSSLER ATTRACTOR BY MEANS OF RESIDUAL AND JOUBERT-GREEFF METHODS

M. C. Kekana, M. Y. Shatalov, T.O Tong and S. E. Fadugba*

Tshwane University of Technology,
Arcadia Campus, Pretoria, SOUTH AFRICA

E-mail : kekanamc@tut.ac.za

*Department of Mathematics,
Ekiti State University, Ado Ekiti, NIGERIA

(Received: Mar. 09, 2023 Accepted: Jul. 23, 2023 Published: Aug. 30, 2023)

Abstract: In this paper, A mathematical framework of checking accuracy of numerical methods from mathematical software is been developed and investigated. Rössler attractor is used as case study as its analytical solution is non-existence. The algorithms investigated from Mathcad software includes AdamsBDF, Adams, BDF and Runge-Kutta fixed methods. The numerical solutions of each built-in algorithms are compared to well-known Joubert-Greeff method. The estimation of global and local residuals are shown. The graphical results are plotted on an interval of $0 \leq t \leq 150$.

Keywords and Phrases: Rössler attractor , MathCad software, Joubert-Greeff method , global and local residuals.

2020 Mathematics Subject Classification: 74H15, 45G10, 65D32, 65D30, 65G99.

1. Introduction

Rössler system is a system of nonlinear differential equation which was derived and studied to details by Otto Rossler in [4]. These differential equations define are continuous-time dynamical system that exhibit chaotic dynamics associated with fractal properties of the attractor. The original Rossler paper in [4] states that

the Rössler attractor was intended to behave similarly to the Lorenz attractor, but also easy to analyze qualitatively. Furthermore the work of checking accuracy numerical solutions of built-in algorithms from mathematica software was done by [2] using Lorenz system as case study.

This attractor has some similarities to the Lorenz attractor, but simpler and has only one manifold. A prototype equation to the Lorenz model of turbulence contains only one nonlinear term and the flow in state allows for a folded Poincare map.

Many natural and artificial systems are governed by this type of equation, but the original theoretical equations were later found to be useful in modelling equilibrium in chemical reaction [5].

The main aim to this work is to investigate all the numerical solutions of built-in algorithms from mathcad software and compared the results to well-known Joubert-Greeff method. The results for both local and global residuals are shown in tabular and graphical forms.

The general Rössler system is defined as:

$$\begin{aligned}\frac{dx}{dt} &= -y(t) - x(t) \\ \frac{dy}{dt} &= x(t) + ay(t) \\ \frac{dz}{dt} &= b + z(t)(x(t) - c)\end{aligned}\tag{1}$$

with $a = 0.2$, $b = 0.2$ and $c = 5.7$ all positive parameters, and initial conditions $x(0) = x_0 = 0.1$ and $y(0) = y_0 = 0.1$ and $z(0) = z_0 = 0.0035$.

In this case for exact solution for $t \in (0, T)$ Rössler attractor with the following parameters: $a = 0.2$, $b = 0.2$ $c = 5.7$ on a time interval $t \in [0, T = 150]$ is simulated numerically. Initial values are $x_0 = 0.1$, $y_0 = 0.1$ and $z_0 = 0.0035$. The solution of protocol is shown in figure 1.

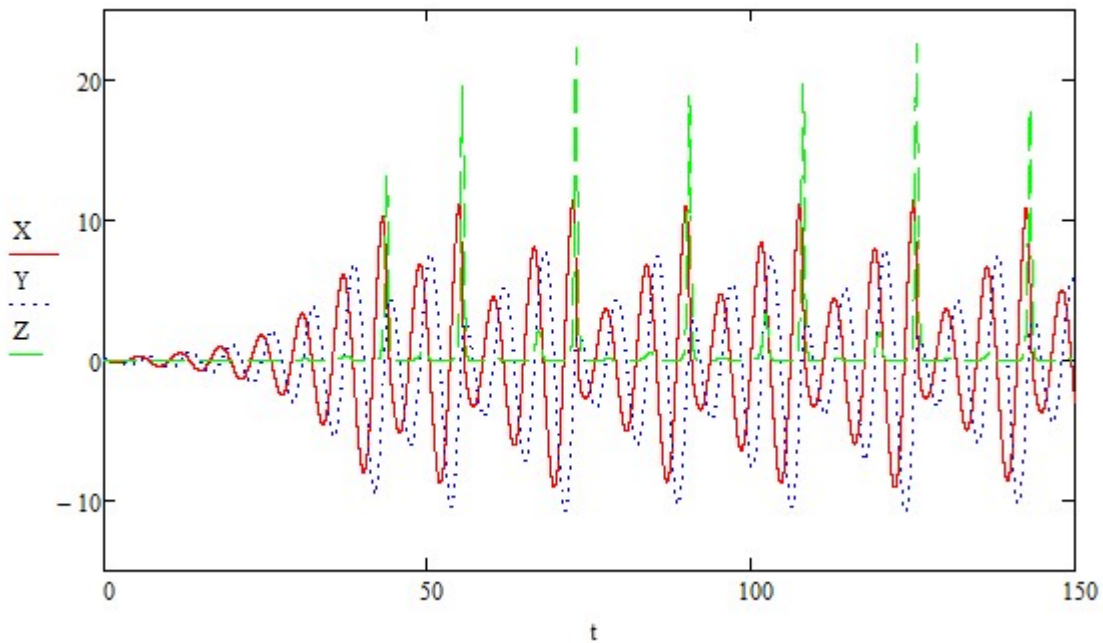


Figure 1: Numerical simulation of $X = x(t)$, $Y = y(t)$, and $Z = z(t)$ with system of equation (1) with $a = 0.2$, $b = 0.2$ and $c = 5.7$ with initial conditions $x(0) = 0.1$, $y(0) = 0.1$ and $z(0) = 0.0035$ by AdamsBDF method with tolerance $\text{Tol} = 10^{-16}$.

Integrating the Rössler system (1), we obtain the following:

$$\begin{aligned}
 x(t) - x_0 + \int_0^t [y(\tau) + z(\tau)] d\tau &= 0, \\
 y(t) - y_0 - \int_0^t [x(\tau) + ay(\tau)] d\tau &= 0, \\
 z(t) - z_0 - bt - \int_0^t [z(\tau)(x(\tau) - c)] d\tau &= 0.
 \end{aligned} \tag{2}$$

The accuracy of numerical solution is measured by residual functions as

$$\begin{aligned}
res_x(t) &= \left| x(t) - x_0 + \int_0^t [y(\tau) + z(\tau)] d\tau \right|, \\
res_y(t) &= \left| y(t) - y_0 - \int_0^t [x(\tau) - ay(\tau)] d\tau \right|, \\
res_z(t) &= \left| z(t) - z_0 - \int_0^t [b + z(\tau)(x(\tau) - c)] d\tau \right|,
\end{aligned} \tag{3}$$

where $x_0 = x(0)$, $y_0 = y(0)$, and $z_0 = z(0)$ and $t \in (0, T)$.

Alternatively using a decimal logarithmic scale as

$$\begin{aligned}
\log [res_x(t)] &= \log \left| x(t) - x_0 + \int_0^t [y(\tau) + z(\tau)] d\tau \right|, \\
\log [res_y(t)] &= \log \left| y(t) - y_0 + \int_0^t [x(\tau) + ay(\tau)] d\tau \right|, \\
\log [res_z(t)] &= \log \left| z(t) - z_0 - bt - \int_0^t [z(\tau)(x(\tau) - c)] d\tau \right|,
\end{aligned} \tag{4}$$

time interval $(0, T)$. The residual introduced in systems of equations (3) and (4) are the global estimations of the accuracy because they relate any time instant $t \in (0, T)$ to original time instant $t = 0$. It is worthwhile to introduce local residual measures of accuracy as follows:

$$\begin{aligned}
res\Delta_x(t_j) &= \left| x(t_j) - x(t_{j-1}) + \int_{t_{j-1}}^{t_j} [y(\tau) + z(\tau)] d\tau \right|, \\
res\Delta_y(t_j) &= \left| y(t_j) - y(t_{j-1}) - \int_{t_{j-1}}^{t_j} [x(\tau) - ay(\tau)] d\tau \right|, \\
res\Delta_z(t_j) &= \left| z(t_j) - z(t_{j-1}) - b(t_j - t_{j-1}) - \int_{t_{j-1}}^{t_j} [z(\tau)(x(\tau) - c)] d\tau \right|,
\end{aligned} \tag{5}$$

and decimal logarithmic measures of the local accuracy for $j = 1, 2, \dots, N$ so that $t_N = T$.

$$\begin{aligned} \log [\text{res}\Delta_x(t_j)] &= \log \left| x(t_j) - x(t_{j-1}) + \int_{t_{j-1}}^{t_j} [y(\tau) + z(\tau)] d\tau \right|, \\ \log [\text{res}\Delta_y(t_j)] &= \log \left| y(t_j) - y(t_{j-1}) - \int_{t_{j-1}}^{t_j} [x(\tau) - ay(\tau)] d\tau \right|, \\ \log [\text{res}\Delta_z(t_j)] &= \log \left| z(t_j) - z(t_{j-1}) - b(t_j - t_{j-1}) - \int_{t_{j-1}}^{t_j} [z(\tau)(x(\tau) - c)] d\tau \right|, \end{aligned} \quad (6)$$

Results of super smoothing are calculated using the built-in function supsmooth in Mathcad. For the global accuracy measures as

$$\begin{aligned} &\underline{\text{supsmooth}} \left(x(t) - x_0 + \int_0^t [y(\tau) + z(\tau)] d\tau \right), \\ &\underline{\text{supsmooth}} \left(y(t) - y_0 - \int_0^t [x(\tau) - ay(\tau)] d\tau \right) \\ &\underline{\text{supsmooth}} \left(z(t) - z_0 - \int_0^t [b + z(\tau)(x(\tau) - c)] d\tau \right), \end{aligned}$$

For the local accuracy measures

$$\begin{aligned} &\underline{\text{supsmooth}} \left(x(t_j) - x(t_{j-1}) + \int_{t_{j-1}}^{t_j} [y(\tau) + z(\tau)] d\tau \right), \\ &\underline{\text{supsmooth}} \left(y(t_j) - y(t_{j-1}) - \int_{t_{j-1}}^{t_j} [x(\tau) - ay(\tau)] d\tau \right), \\ &\underline{\text{supsmooth}} \left(z(t_j) - z(t_{j-1}) - b(t_j - t_{j-1}) - \int_{t_{j-1}}^{t_j} [z(\tau)(x(\tau) - c)] d\tau \right), \end{aligned}$$

or the decimal logarithm of modulus of these measures. The super smooth function returns a vector created by a piece-wise application of symmetric neighbor linear least-squares fitting on each element of ordinates in which the number of nearest neighbors is chosen adaptively. The super smooth function performs a fast algorithm that uses adaptive window to calculate a localized linear fit to the data. This function takes time data in strictly increasing order and implements a fast algorithm which can observe a periodic trend in the data. The super smoothing is particular useful in the case where data has different noise components at different time intervals. For realization of the Joubert-Greeff method we introduce modified Rössler's system of sixth order by means of differentiation of original Rössler's system (1):

$$\begin{aligned}\frac{dx(t)}{dt} &= u(t), \quad \frac{dy(t)}{dt} = v(t), \quad \frac{dz(t)}{dt} = w(t), \\ \frac{du(t)}{dt} &= -v(t) - w(t), \\ \frac{dv(t)}{dt} &= u(t) + av(t), \\ \frac{dw(t)}{dt} &= -cw(t) + u(t)z(t) + x(t)w(t)\end{aligned}\tag{7}$$

with initial conditions $x(0) = x_0, y(0) = y_0, z(0) = z_0, u(0) = u_0 = -y_0 - z_0, v(0) = v_0 = x_0 + a.y_0, w(0) = w_0 = b + z_0(x_0 - c)$. Assuming that the solution of this IVP is $\tilde{x} = \tilde{x}(t), \tilde{y} = \tilde{y}(t), \tilde{z} = \tilde{z}(t)$, in accordance with the Joubert-Greeff method the error of numerical solution of the IVPs is calculated as difference between solutions of IVP (1) and (7):

$$J\Delta x(t) = |x(t) - \tilde{x}(t)|, J\Delta y(t) = |y(t) - \tilde{y}(t)|, J\Delta z(t) = |z(t) - \tilde{z}(t)|\tag{8}$$

or considering in the decimal logarithmic measures:

$$\begin{aligned}LJ\Delta x(t_j) &= |\log(J\Delta x(t_j))|, \\ LJ\Delta y(t_j) &= |\log(J\Delta y(t_j))|, \\ LJ\Delta z(t_j) &= |\log(J\Delta z(t_j))|,\end{aligned}\tag{9}$$

2. Comparison of Numerical Procedures using Mathcad15 on Rössler System

In this section, the maximum values of the global, local residuals and maximum values of the Joubert-Greeff difference functions for solutions obtained by different Mathcad built-in solvers on time interval $t \in [0, 150]$ are analyzed. On that interval $N = 50 \times 10^3$ sub-intervals is selected so the step-size is equal to $h = \frac{150}{50 \times 10^3} = 3 \times 10^{-3}$. Another peculiarity of the residual method is that we eliminated intermediate interpolation of solutions and used the Gauss integration in three intermediate points.

Method	$\max 10^{LSx_j}$	$\max 10^{L\Delta x_j}$	$\max 10^{LJ\Delta x_j}$
AdamsBDF	$10^{-8.1}$	$10^{-10.5}$	$10^{-6.9}$
Adams	$10^{-7.1}$	$10^{-10.1}$	$10^{-6.3}$
BDF	$10^{-7.3}$	$10^{-10.3}$	$10^{-5.6}$
RKfixed	$10^{-10.7}$	$10^{-12.4}$	$10^{-7.2}$
RKadapt	$10^{-11.8}$	$10^{-12.2}$	$10^{-9.3}$
Bulstoer	$10^{-11.8}$	$10^{-11.8}$	$10^{-9.2}$
Radau	$10^{-9.5}$	$10^{-11.9}$	$10^{-9.3}$
Stiffb	$10^{-11.1}$	$10^{-12.2}$	$10^{-10.2}$
Stiffr	$10^{-9.8}$	$10^{-11.7}$	$10^{-9.4}$

Table 1: Local, global residuals together with Joubert-Greeff method on x -component

Method	$\max 10^{LSy_j}$	$\max 10^{L\Delta y_j}$	$\max 10^{LJ\Delta y_j}$
AdamsBDF	$10^{-7.1}$	$10^{-10.5}$	$10^{-7.1}$
Adams	$10^{-7.0}$	$10^{-10.3}$	$10^{-6.2}$
BDF	$10^{-7.0}$	$10^{-10.3}$	$10^{-5.6}$
RKfixed	$10^{-12.0}$	$10^{-12.8}$	$10^{-7.3}$
RKadapt	$10^{-12.5}$	$10^{-12.5}$	$10^{-9.5}$
Bulstoer	$10^{-11.7}$	$10^{-12.2}$	$10^{-9.2}$
Radau	$10^{-9.7}$	$10^{-12.2}$	$10^{-9.4}$
Stiffb	$10^{-11.5}$	$10^{-12.5}$	$10^{-10.2}$
Stiffr	$10^{-9.8}$	$10^{-11.8}$	$10^{-9.5}$

Table 2: Local, global residuals together with Joubert-Greeff method on y -component

Method	$\max 10^{LSz_j}$	$\max 10^{L\Delta z_j}$	$\max 10^{LJ\Delta z_j}$
AdamsBDF	$10^{-7.7}$	$10^{-9.8}$	$10^{-6.5}$
Adams	$10^{-7.8}$	$10^{-9.4}$	$10^{-5.8}$
BDF	$10^{-7.4}$	$10^{-9.7}$	$10^{-5.2}$
RKfixed	$10^{-10.3}$	$10^{-12.2}$	$10^{-6.7}$
RKadapt	$10^{-11.2}$	$10^{-11.8}$	$10^{-8.9}$
Bulstoer	$10^{-11.3}$	$10^{-11.7}$	$10^{-8.6}$
Radau	$10^{-9.4}$	$10^{-11.5}$	$10^{-8.8}$
Stiffb	$10^{-10.9}$	$10^{-11.9}$	$10^{-9.7}$
Stiffc	$10^{-10.0}$	$10^{-11.2}$	$10^{-9.9}$

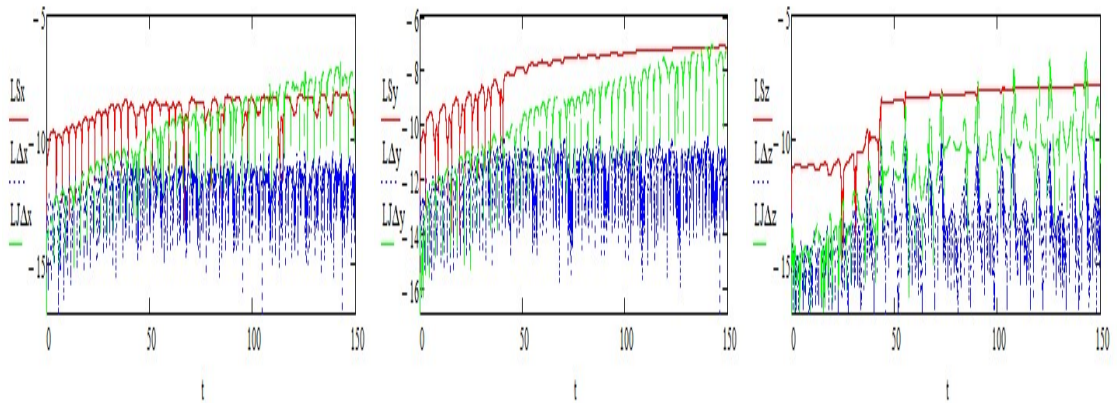
Table 3: Local, global residuals together with Joubert-Greeff method on z -component

Tables 1 to 3 indicates that

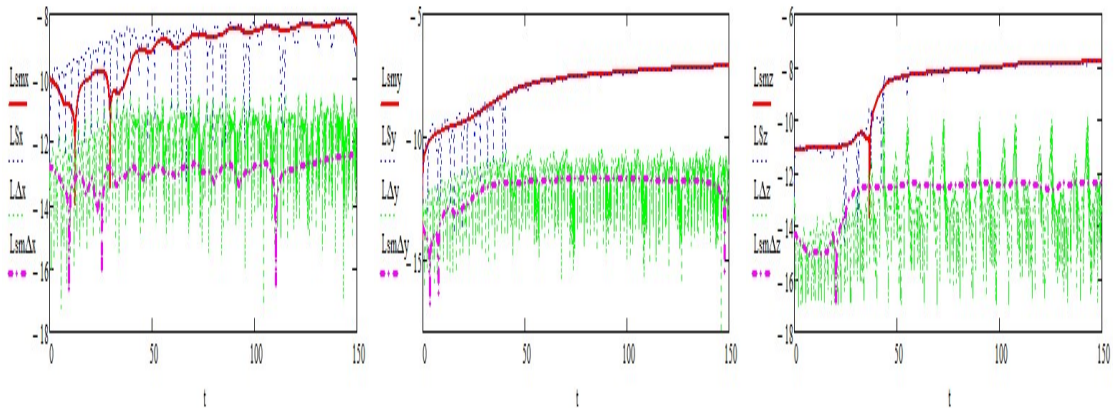
- Backward differential formula (BDF) gives worse approximation for all three components $x(t)$, $y(t)$ and $z(t)$.
- The best accuracy for numerical solution is given by Runge-Kutta adapt method for $x(t)$ component with values $10^{-11.8}$ for global residual and $10^{-12.2}$ for local residuals.
- Joubert-Greeff method is showing divergence when Backward differential formula is used across all the three components.

3. Graphical Results

Both global and local methods of residual functions will be used in what will follow and results will be compared with well known method in [1] difference methods evaluated in (1) to (7). The Rössler system is considered with parameters $a = 0.2, b = 0.2$ and $c = 5.7$ and the results of both local and global errors of super-smoothing are shown. In both residual measures the same initial conditions will be considered $x_0 = 0.1, y_0 = 0.1$ and $z_0 = 0.0035$. In figures 2 - 10, the results of super smoothing are shown to obtain averaged results of both local and global residuals. LSx, LSy, LSz and $L\Delta x, L\Delta y, L\Delta z$ represents both global and local residual estimations for x, y, z -components from the investigated Rössler's system. $LJ\Delta x, LJ\Delta y, LJ\Delta z$ are the estimations using the Joubert-Greeff method for x, y, z -components.

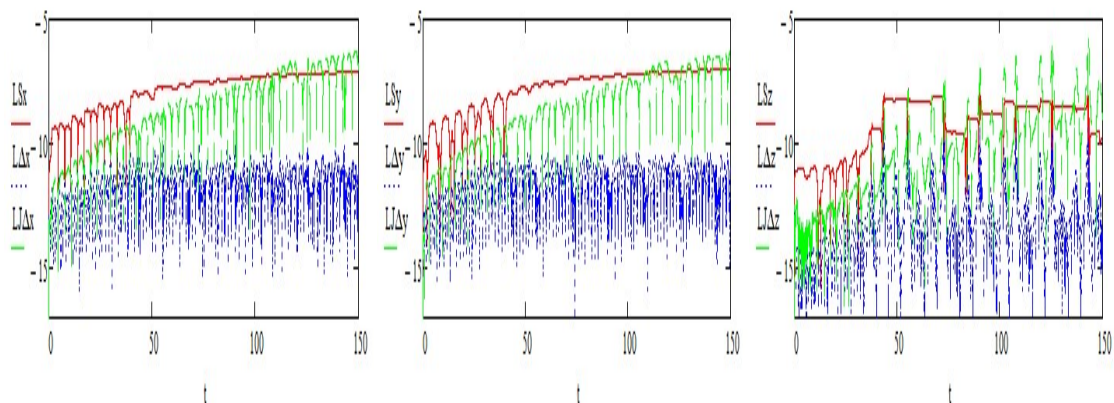


(a) The global and local residual for x component (b) The global and local residual for y component (c) The global and local residual for z component

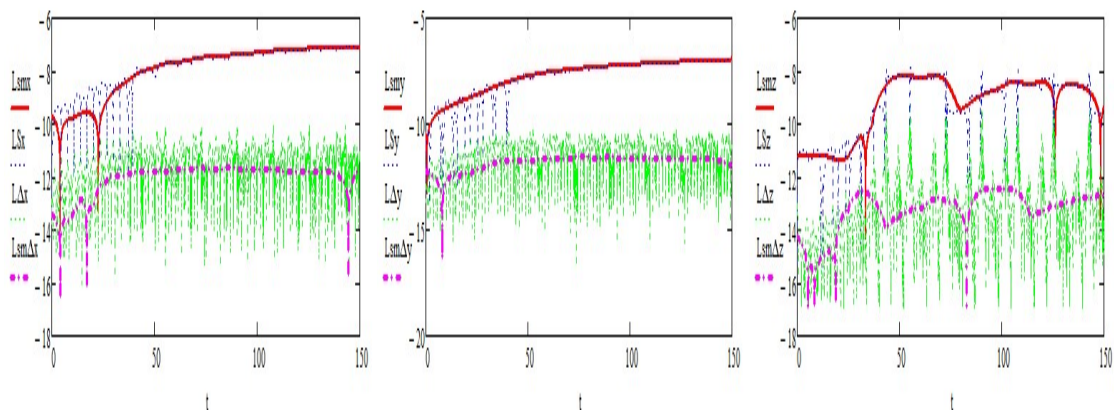


(d) Super-smoothed local and global residual for x component (e) Super-smoothed local and global residual for y component (f) Super-smoothed local and global residual for z component

Figure 2: The six graphs were plotted using AdamsBDF method with $x(0) = 0.1$, $y(0) = 0.1$ and $z(0) = 0.0035$ for both local, global errors and Joubert-Greeff method of checking accuracy. The results of super-smoothing function was applied to obtain clear results of both local and global error.

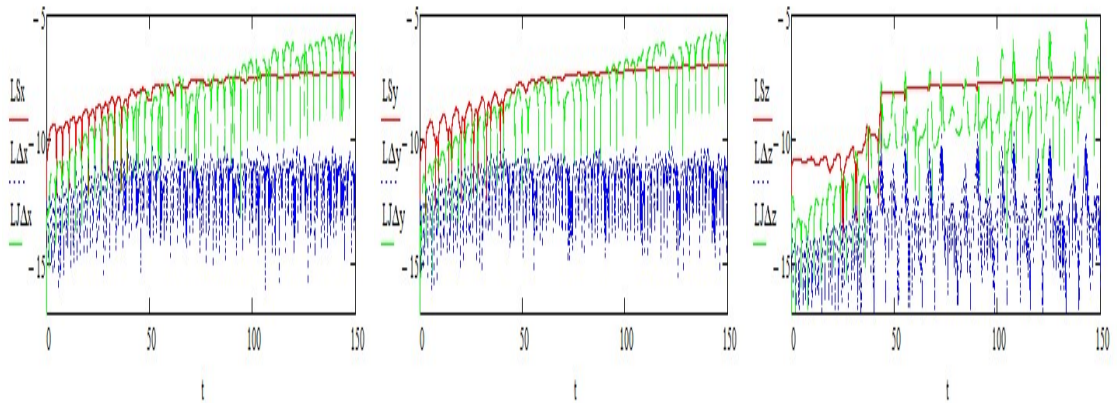


(a) The global and local residual for x component (b) The global and local residual for y component (c) The global and local residual for z component

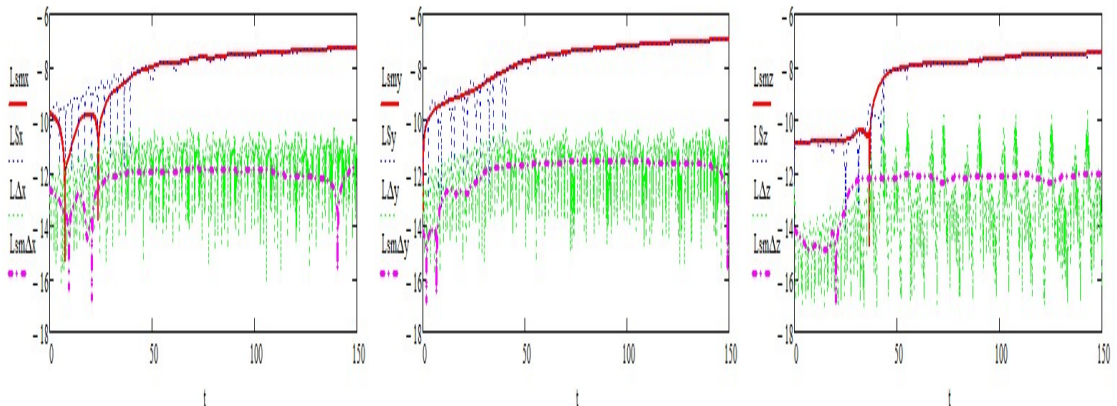


(d) Super-smoothed local and global residual for x component (e) Super-smoothed local and global residual for y component (f) Super-smoothed local and global residual for z component

Figure 3: The six graphs were plotted using Adams method with $x(0) = 0.1$, $y(0) = 0.1$ and $z(0) = 0.0035$ for both local, global errors and Joubert-Greeff method of checking accuracy. The results of super-smoothing function was applied to obtain clear results of both local and global error.

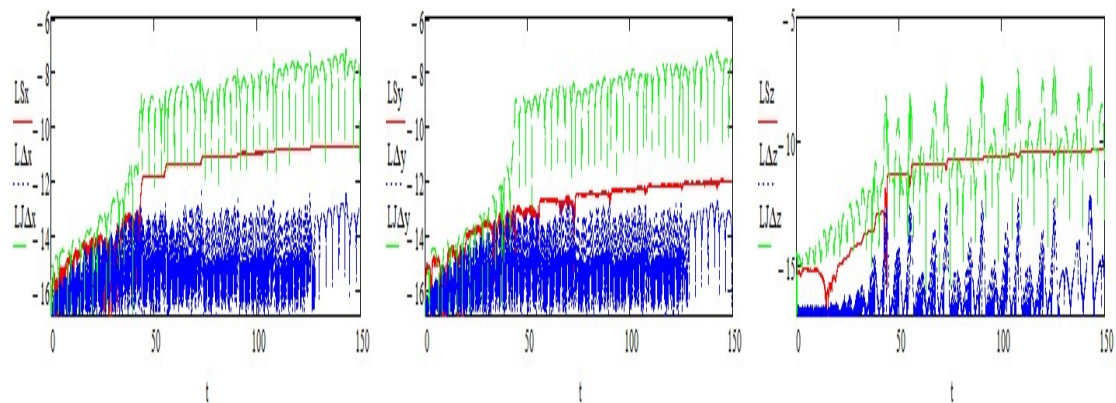


(a) The global and local residual for x component (b) The global and local residual for y component (c) The global and local residual for z component

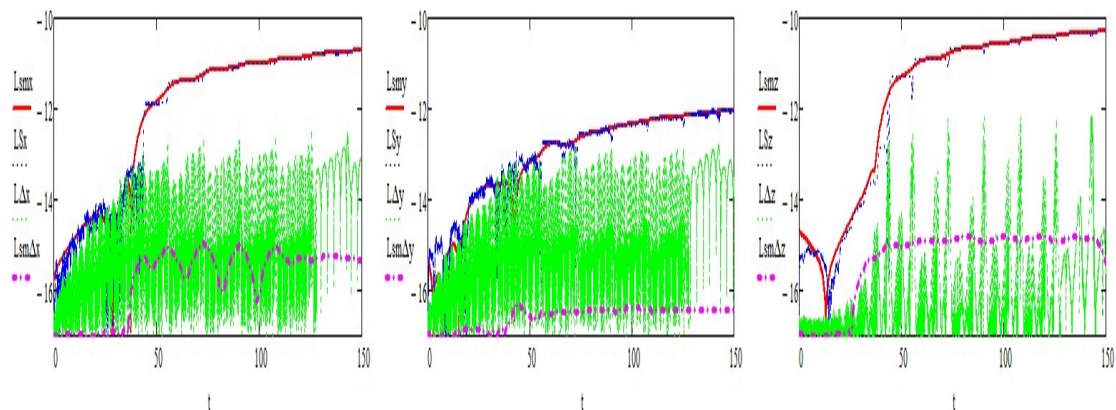


(d) Super-smoothed local and global residual for x component (e) Super-smoothed local and global residual for y component (f) Super-smoothed local and global residual for z component

Figure 4: The six graphs were plotted using BDF method with $x(0) = 0.1$, $y(0) = 0.1$ and $z(0) = 0.0035$ for both local, global errors and Joubert-Greff method of checking accuracy. The results of super-smoothing function was applied to obtain clear results of both local and global error.

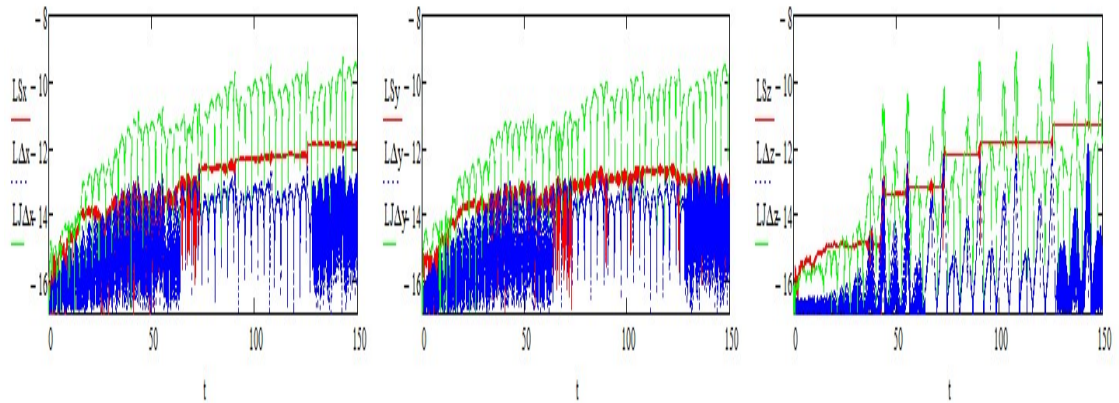


(a) The global and local residual for x component (b) The global and local residual for y component (c) The global and local residual for z component

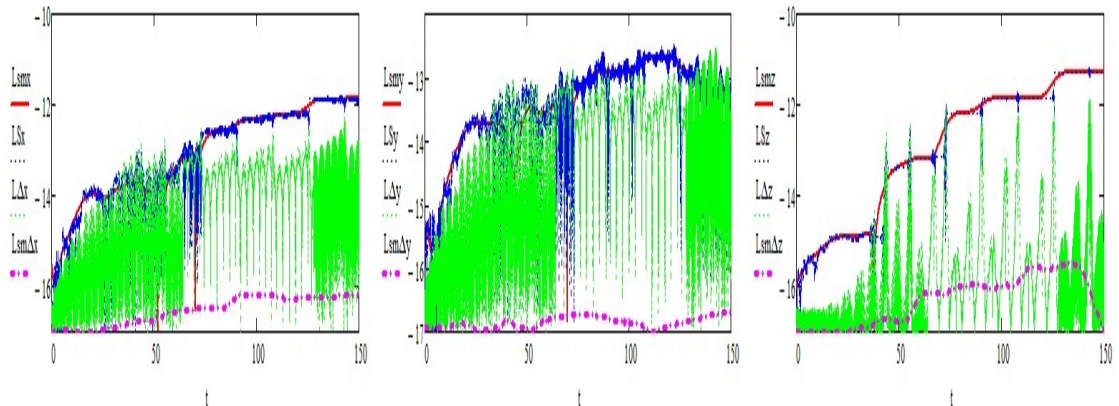


(d) Super-smoothed local and global residual for x component (e) Super-smoothed local and global residual for y component (f) Super-smoothed local and global residual for z component

Figure 5: The six graphs were plotted using Runge-Kutta fixed method with $x(0) = 0.1$, $y(0) = 0.1$ and $z(0) = 0.0035$ for both local, global errors and Joubert-Greeff method of checking accuracy. The results of super-smoothing function was applied to obtain clear results of both local and global error.

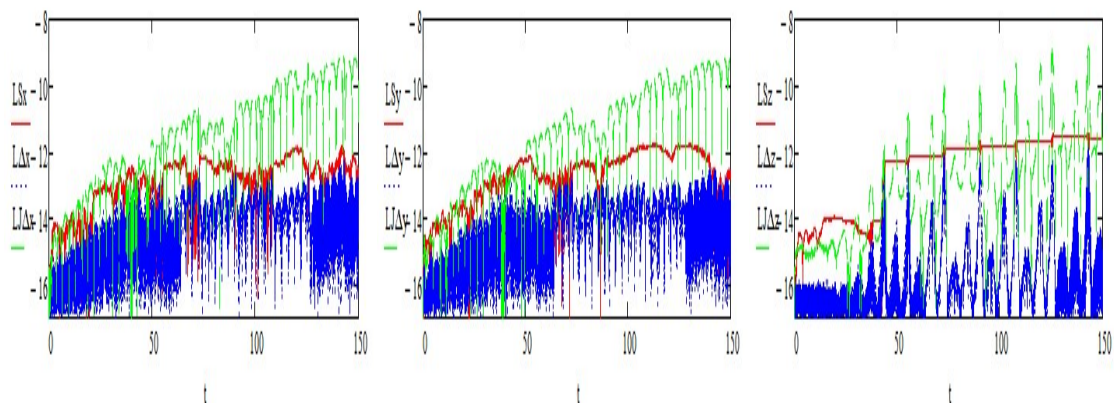


(a) The global and local residual for x component (b) The global and local residual for y component (c) The global and local residual for z component

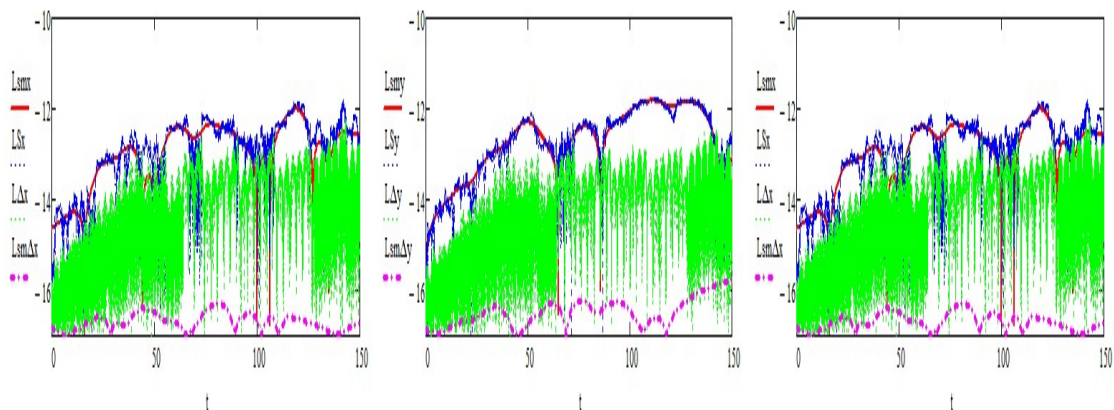


(d) Super-smoothed local and global residual for x component (e) Super-smoothed local and global residual for y component (f) Super-smoothed local and global residual for z component

Figure 6: The six graphs were plotted using Runge-Kutta adapt method with $x(0) = 0.1$, $y(0) = 0.1$ and $z(0) = 0.0035$ for both local, global errors and Joubert-Greeff method of checking accuracy. The results of super-smoothing function was applied to obtain clear results of both local and global error.

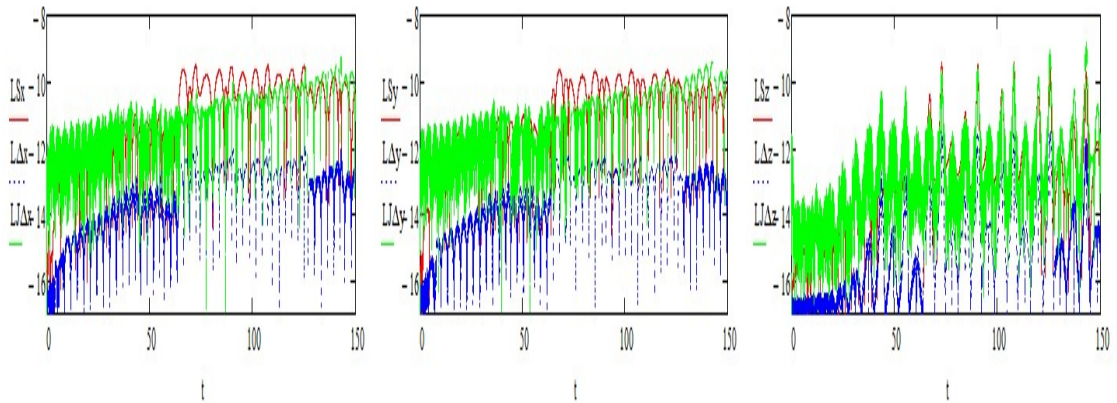


(a) The global and local residual for x component (b) The global and local residual for y component (c) The global and local residual for z component

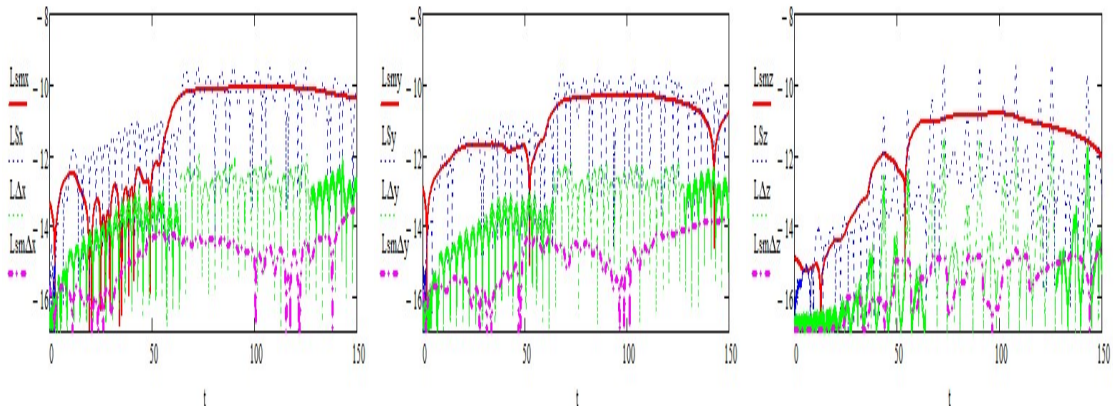


(d) Super-smoothed local and global residual for x component (e) Super-smoothed local and global residual for y component (f) Super-smoothed local and global residual for z component

Figure 7: The six graphs were plotted using Bulstoer method with $x(0) = 0.1$, $y(0) = 0.1$ and $z(0) = 0.0035$ for both local, global errors and Joubert-Greeff method of checking accuracy. The results of super-smoothing function was applied to obtain clear results of both local and global error.

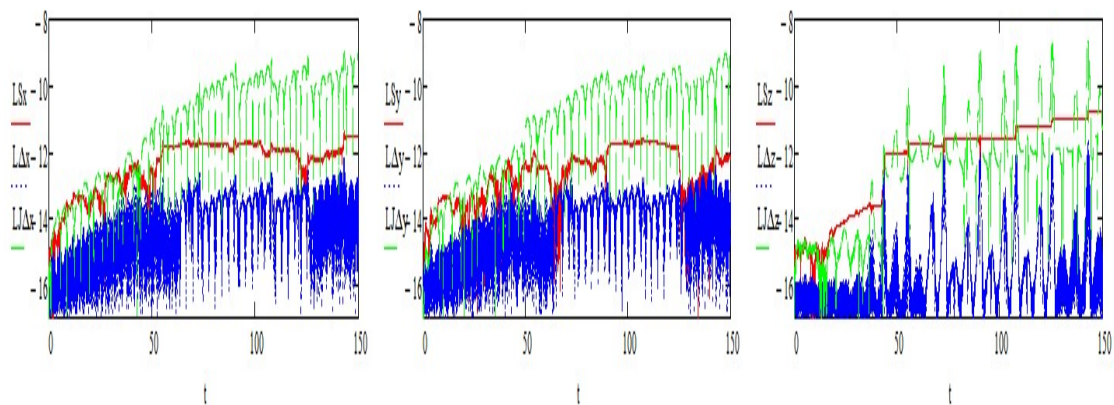


(a) The global and local residual for x component (b) The global and local residual for y component (c) The global and local residual for z component

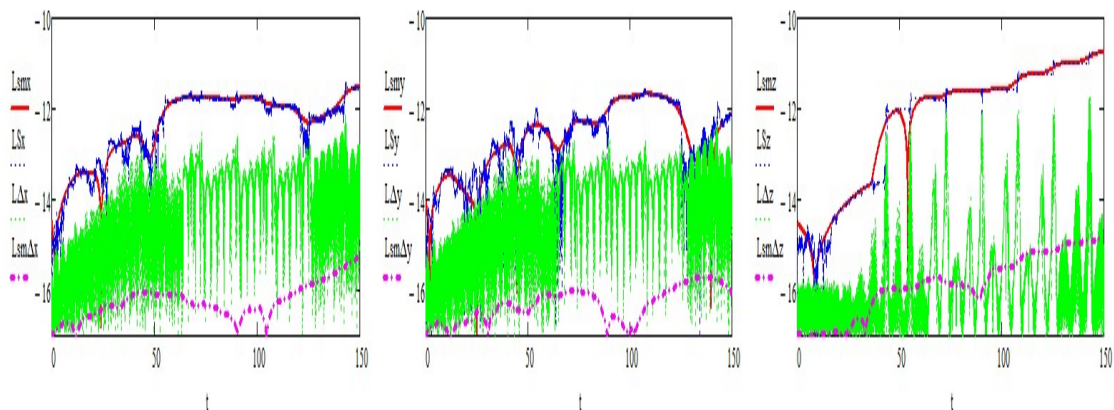


(d) Super-smoothed local and global residual for x component (e) Super-smoothed local and global residual for y component (f) Super-smoothed local and global residual for z component

Figure 8: The six graphs were plotted using Radau method with $x(0) = 0.1$, $y(0) = 0.1$ and $z(0) = 0.0035$ for both local, global errors and Joubert-Greeff method of checking accuracy. The results of super-smoothing function was applied to obtain clear results of both local and global error.

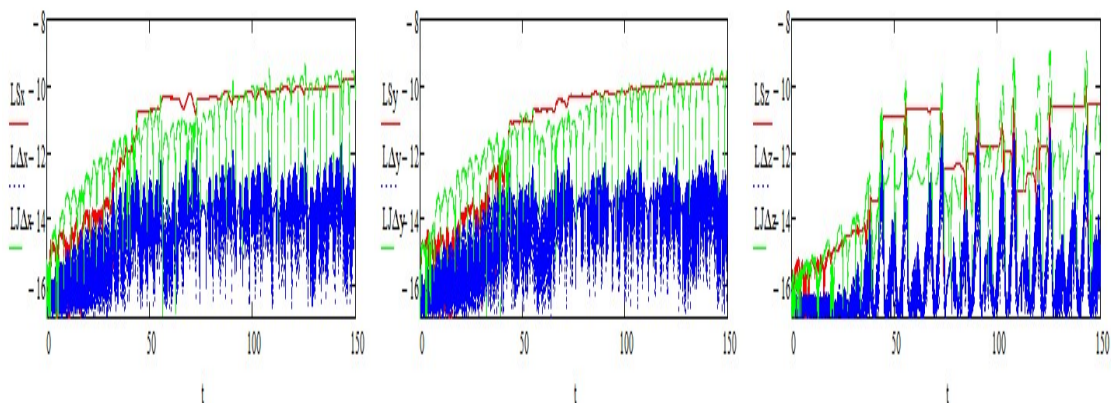


(a) The global and local residual for x component (b) The global and local residual for y component (c) The global and local residual for z component

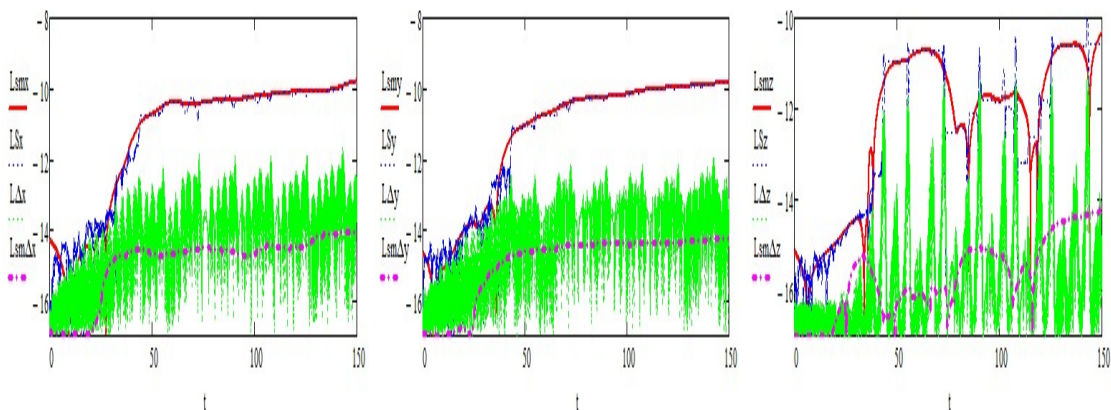


(d) Super-smoothed local and global residual for x component (e) Super-smoothed local and global residual for y component (f) Super-smoothed local and global residual for z component

Figure 9: The six graphs were plotted using Stiff-Bulstoer method with $x(0) = 0.1$, $y(0) = 0.1$ and $z(0) = 0.0035$ for both local, global errors and Joubert-Greeff method of checking accuracy. The results of super-smoothing function was applied to obtain clear results of both local and global error.



(a) The global and local residual for x component (b) The global and local residual for y component (c) The global and local residual for z component



(d) Super-smoothed local and global residual for x component (e) Super-smoothed local and global residual for y component (f) Super-smoothed local and global residual for z component

Figure 10: The six graphs were plotted using Stiff-Radau method with initial conditions $x(0) = 0.1$, $y(0) = 0.1$ and $z(0) = 0.0035$ for both local, global errors and Joubert-Greeff method of checking accuracy. The results of super-smoothing function was applied to obtain clear results of both local and global error.

4. Discussion of graphical results and conclusions

In this paper the intermediate interpolation of discrete solutions is eliminated. It is achieved by means of special selection of points where solutions of the IVPs were determined. These points corresponded to nodes of the Gauss quadrature in-

tegration namely, they coincided with the Gauss three points integration scheme. The z -components of the solutions of the Rössler attractor characterized by sharp positive spikes. Due to presence of these spikes in z -components of the solutions corresponding local residuals were also characterized by sharp spikes of approximately two orders of magnitude higher than the local residuals between spikes. Maximum values of the local residuals grown in time. Due to the sharp spikes of the local residuals the global residuals functions demonstrated a "ladder"-behaviour. This behaviour is especially evident in the global residuals of the most accurate solutions, for example, the solution obtained by the Runge-Kutta 4 solver with adaptive step-size.

The growth of the residual functions of the z -component of the solutions is explained by presence of larger values of higher derivatives in vicinity of the spikes. The trend of residuals to increase with time is explained by the fact that positive and negative values of the higher derivatives did not compensated each other, hence stipulating the drifts of the residual functions. The Joubert-Greeff differences also demonstrated sharp spikes. These spikes were well correlated with the spikes of the z -components of the solutions. These differences demonstrated substantial growth with time which was several orders of magnitude higher than the growth of the global residuals. The developed method of accuracy estimation by the local and global residuals demonstrated its advantage in comparison with the known Joubert-Greeff method in analysis of the Rössler attractor.

Acknowledgement

The author(s) wishes to thank the Tshwane university of Technology for their financial support.

References

- [1] Joubert, S. V., Greeff, J. C., Accuracy estimates for computer algebra system initial-value problem (IVP) solvers, *South African Journal of Science*, 102 (1), (2006), 46-50.
- [2] Kekana, M. C., Tong, T. O., Shatalov, M. Y., and Moshokoa, S. P., Accuracy test on built-in algorithms applied to the Lorenz system, *Journal of Computational and Theoretical Nanoscience*, 16 (10), (2021), 4064-4071.
- [3] Pierper, R. J., Blair, D. J., A practical solution to the numerical butterfly effects in chaotic system for fast but memory limited computers, 2010, 42nd Southeastern symposium on system theory, University of Texas, USA.

- [4] Rossler, O. E., An equation of contineous chaos, *Physics Letters*, 57A (5), (1976), 397-398.
- [5] Rossler, O.E., Chaos behaviour in simple reaction system, *Z Naturforsch, A*, (31), (1976), 259-264.

This page intentionally left blank.